

THE NUMERICAL EXPERIMENTS ON APPLYING GEOSTROPHIC MOMENTUM APPROXIMATION TO THE BAROCLINIC AND NON-NEUTRAL PBL

Zhao Ming (赵 鸣)

Department of Atmospheric Sciences, Nanjing University, Nanjing

Received June 2, 1987

ABSTRACT

In this paper, Wu and Blumen's boundary layer geostrophic momentum approximation model (Wu and Blumen, 1982) is applied to baroclinic and non-neutral PBL, the motion equations for the PBL under the geostrophic momentum approximation are solved, in which the eddy transfer coefficient is a function of the distributions of the wind and temperature. The results are compared with those in barotropic and neutral conditions with the geostrophic momentum approximation. It is found that in the baroclinic condition, the wind distribution has both the characteristics of a steady, homogeneous and baroclinic PBL and those caused by the geostrophic momentum approximation. Those in non-neutral conditions show that they retain the intrinsic characteristics for the wind in non-neutral PBL, at the same time, the effects of the large-scale advection and local variation are also included. We can predict the wind in the non-neutral and baroclinic PBL by use of the geostrophic momentum approximation when the temporal and spatial distributions of the geostrophic wind, as well as the potential temperatures and their variation rates at the upper and lower boundary of the PBL are given by large-scale model. Finally, the model is extended to the case over sea surface.

1. INTRODUCTION

Zhao (1988) had performed the numerical experiments for the motion in the barotropic and neutral PBL utilizing Wu and Blumen's boundary layer geostrophic momentum approximation model (Wu and Blumen, 1982) but with the eddy transfer coefficient as a function of the vertical shear of the wind, the reasonable and actual wind distributions were obtained. The application of the geostrophic momentum approximation to the PBL is connected with some practical problems such as to predict the wind in the PBL based on the wind predicted at the top of the PBL from the large scale model. Previously, the wind in the PBL was diagnosed or interpolated from the wind at the top of the PBL based on the steady and homogeneous PBL model. The shortcoming of this method is that the effects of local variation and advection cannot be included. Wu and Blumen (1982) applied the geostrophic momentum approximation to the PBL, the primary three dimensional motion equations for the PBL had been linearized in which the local and advective variations of the geostrophic wind could be learned from the large scale model. Hence, the original three dimensional model became one dimensional, its solution could give the wind distribution in the PBL from the wind at the top of the PBL, the accuracy had been raised because the effects of the local and advective variations had been considered. Zhao (1988) obtained more reasonable and actual results by use of the nonlinear K expression which was usually used in modern PBL models instead of the constant K in Wu and

Blumen's work. But the boundary layer was assumed to be neutral and barotropic in that work, in reality, the PBL usually is baroclinic and non-neutral, the purpose of this paper is to extend Zhao's work to the baroclinic and non-neutral conditions. A series of numerical experiments show that the geostrophic momentum approximation may be applied successfully to the baroclinic and non-neutral PBL which gives a more reasonable and reliable method to predict the wind in the PBL from the large scale model.

Qin et al. (1986) and Liu and Qin (1986) applied the geostrophic momentum approximation to the baroclinic and non-neutral PBL, but their PBL model was the classical two layer model, i. e., $K = \text{const}$ was used above the surface layer, in the surface layer the known wind and temperature profiles were applied. Theoretically, the scheme taking $K = \text{const}$ in the Ekman layer is not rigorous (Deardorff et al, 1982), which is not applied in modern numerical models for the PBL except some dynamics studies. In this paper, the numerical experiments are done for applying the geostrophic momentum approximation to the baroclinic and non-neutral PBL with the assumption that the eddy transfer coefficient is a function of the vertical distributions of wind and temperature. Finally, the model is extended to the case over sea surface.

II. EXPERIMENTS FOR APPLYING THE GEOSTROPHIC MOMENTUM APPROXIMATION TO THE BAROCLINIC PBL

The motion equations for the PBL with the geostrophic momentum approximation may be written as (Wu and Blumen, 1982):

$$\frac{\partial u_g}{\partial t} - u \frac{\partial u_g}{\partial x} + v \frac{\partial u_g}{\partial y} = f(v - v_g) + \frac{\partial}{\partial z} K \frac{\partial u}{\partial z}, \quad (1)$$

$$\frac{\partial v_g}{\partial t} + u \frac{\partial v_g}{\partial x} + v \frac{\partial v_g}{\partial y} = -f(u - u_g) + \frac{\partial}{\partial z} K \frac{\partial v}{\partial z}, \quad (2)$$

where u_g and v_g are the geostrophic wind components; u and v , the wind components. We assume that the PBL is baroclinic and neutral (the case for baroclinic and non-neutral will be discussed below), for which the following K expression may be used as Zhao (1988):

$$K = l^2 \left[\left(\frac{\partial u}{\partial z} \right)^2 + \left(\frac{\partial v}{\partial z} \right)^2 \right]^{\frac{1}{2}} \quad (3)$$

l is mixing length:

$$l = \frac{0.4(z + z_0)}{1 + \frac{0.4(z + z_0)}{\lambda}} \quad (4)$$

$$\lambda = \frac{0.0063 u_*}{f} \quad (5)$$

z_0 is the roughness of ground, u_* the friction velocity determined by

$$u_* = \left(K \left| \frac{dV}{dz} \right| \right)_{z=z_s}^{\frac{1}{2}} \quad (6)$$

z_s is a height in the surface layer, $z_s = 1$ cm is taken in this paper to represent the smooth surface, we can investigate the effects of the z_0 if other z_s are taken. $f = 10^{-4} \text{ s}^{-1}$

is taken for middle latitudes. In the baroclinic PBL, u_g and v_g are the functions of height which can be found from large scale model. For example, the geostrophic wind field at different heights in the PBL may be interpolated from the predicted pressure fields at 850 hPa and surface. At present, the u_g and v_g in Eqs. (1) and (2) are treated as known functions of the height. Eqs. (1)–(6) form a closed set and the numerical method for solving them is the same as given by Zhao (1988). The upper boundary condition is the same as that paper, i. e.,

$$u = u_\tau, \quad v = v_\tau \quad \text{where } z = h = 1000 \text{ m}, \tag{7}$$

here,

$$u_\tau = \frac{\left(u_g - \frac{1}{f} \frac{\partial v_g}{\partial t}\right) \left(1 - \frac{1}{f} \frac{\partial u_g}{\partial y}\right) - \left(v_g + \frac{1}{f} \frac{\partial u_g}{\partial t}\right) \frac{1}{f} \frac{\partial v_g}{\partial y}}{\left(1 + \frac{1}{f} \frac{\partial v_g}{\partial x}\right) \left(1 - \frac{1}{f} \frac{\partial u_g}{\partial y}\right) + \frac{1}{f^2} \frac{\partial u_g}{\partial x} \frac{\partial v_g}{\partial y}} \tag{8}$$

$$v_\tau = \frac{\frac{1}{f} \left(u_g - \frac{1}{f} \frac{\partial v_g}{\partial t}\right) \frac{\partial u_g}{\partial x} + \left(v_g + \frac{1}{f} \frac{\partial u_g}{\partial t}\right) \left(1 + \frac{1}{f} \frac{\partial v_g}{\partial x}\right)}{\left(1 + \frac{1}{f} \frac{\partial v_g}{\partial x}\right) \left(1 - \frac{1}{f} \frac{\partial u_g}{\partial y}\right) + \frac{1}{f^2} \frac{\partial u_g}{\partial x} \frac{\partial v_g}{\partial y}} \tag{9}$$

As an example, the vertical distribution of the geostrophic wind in the PBL is assumed to be:

$$v_g = v_{gh} \tag{10}$$

$$u_g = u_{gh} - C(h - z) \tag{11}$$

$$C = \pm 3 \times 10^{-3} \text{ s}^{-2}, \tag{12}$$

where $u_{gh} = 10 \text{ m/s}$, $v_{gh} = 0$ are their values at the top of the PBL, in Eq. (12), '+' represents that the geostrophic wind speed increases with height, the reverse is true for '-'. Assuming the horizontal distribution of the geostrophic wind is homogeneous but the temporal tendency of the geostrophic wind does not vanish, then we may apply the geostrophic momentum approximation.

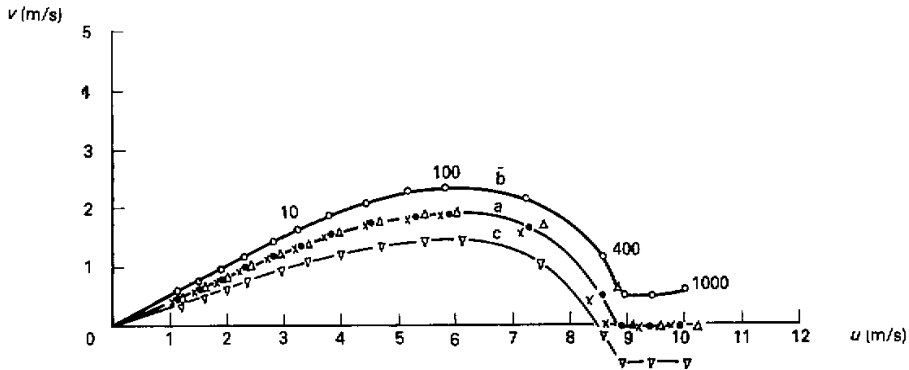


Fig. 1. The wind distribution for the case that the geostrophic wind increases with height under the assumption of geostrophic momentum approximation,

- the steady, homogeneous solutions (curve a);
- $\partial u_g / \partial t = 5 \text{ m s}^{-1} / 24 \text{ h}$; (curve b);
- × $\partial v_g / \partial t = 2 \text{ m s}^{-1} / 24 \text{ h}$;
- ▽ $\partial u_g / \partial t = -5 \text{ m s}^{-1} / 24 \text{ h}$ (curve c);
- △ $\partial v_g / \partial t = -2 \text{ m s}^{-1} / 24 \text{ h}$.

The lower boundary condition is:

$$u = v = 0, \quad \text{where } z = 0. \tag{13}$$

Assuming $\frac{\partial u_g}{\partial t} = \pm 5 \text{ m s}^{-1}/24 \text{ h}$, $\frac{\partial v_g}{\partial t} = \pm 2 \text{ m s}^{-1}/24 \text{ h}$, we solve the Eqs. (1)-(6) for these cases. The vertical grid system is the same as Zhao (1988). The results of the wind distribution are shown in Figs. 1 and 2.

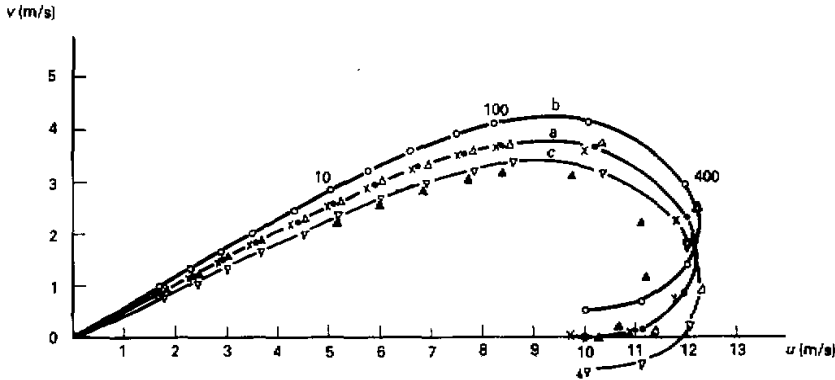


Fig. 2. The wind distribution for the case that the geostrophic wind decreases with height under the assumption of geostrophic momentum approximation, the legend is identical to Fig. 1, and \blacktriangle are the results beginning from 10 m for $\theta_k = -10^\circ$, $\theta_0 = 0^\circ$, $\partial u_g / \partial t = -5 \text{ m s}^{-1}/24 \text{ h}$.

Curve a illustrates the solutions for $\partial u_g / \partial t = \partial v_g / \partial t = 0$, i. e. the steady and baroclinic PBL. It is shown that in the case of $\partial u_g / \partial t > 0$, v are greater than that in the case of $\partial u_g / \partial t = 0$, i. e., the steady and homogeneous solutions both when the geostrophic wind increases and decreases with height, the reverse is true for $\partial u_g / \partial t < 0$. In the case of $\partial v_g / \partial t > 0$, u are less than that in the case of $\partial v_g / \partial t = 0$ (steady, homogeneous solutions) both when the geostrophic wind increases and decreases with height, the reverse is true for $\partial v_g / \partial t < 0$. The reason is similar to that shown by Zhao (1988), in the case of $\partial u_g / \partial t > 0$, it is equivalent to putting $\partial u_g / \partial t = 0$ in Eq. (1) and at the same time to make the $-fv_g$ on the right hand side decrease, i. e., make v_g increase, this results in the increase of v ; the cases for $\partial u_g / \partial t < 0$ and $\partial v_g / \partial t \geq 0$ can also be explained similarly. Therefore, the baroclinity does not change the effect of the local variation on the wind distribution in the PBL. Similarly, we can analogize that the baroclinity can not change the effect of advection on the wind distribution in the PBL. In other words, the geostrophic momentum approximation may be applied successfully in the baroclinic condition. The differences for the vertical distributions of the wind in Figs. 1 and 2 in the case of the same $\partial u_g / \partial t$ or $\partial v_g / \partial t$ are caused by the different baroclinities (i. e., caused by the differences between two curves (a) in these figures). In Fig. 1, the fact that the spirals extend along the direction of x axis and do not intersect with the x axis when the height increases is the intrinsic characteristic for the baroclinic PBL, see for example, Estoque (1973).

III. THE EXPERIMENTS FOR APPLYING GEOSTROPHIC MOMENTUM APPROXIMATION TO THE NON-NEUTRAL PBL

Assume that the PBL is barotropic but non-neutral, the temperature stratification will affect the eddy transfer coefficient. In modern numerical models for the PBL, when we calculate the wind distribution in the non-neutral PBL theoretically, the distribution of potential temperature $\partial\theta/\partial z$ in the PBL is usually assumed to be known, then we can solve the motion equations for the PBL and get the wind distribution. In order to show the differences between the solutions with the geostrophic momentum approximation and the steady, homogeneous solutions, we solve the motion equations for the PBL with the geostrophic momentum approximation and without it, i. e., with the steady and homogeneous condition under the same $\partial\theta/\partial z$, from which we can find the effect of the geostrophic momentum approximation to the non-neutral PBL. In the numerical experiments, different values may be taken for $\partial\theta/\partial z$, as an example, in this paper, the $\partial\theta/\partial z$ distribution derived from solving the thermodynamics equation and motion equations in the steady and homogeneous PBL simultaneously with the known potential temperatures at the top and bottom of the PBL is taken to solve the motion equations for the PBL with the geostrophic momentum approximation. Then the comparison between the solutions with and without the geostrophic momentum approximation may show the effect of the geostrophic momentum approximation to the non-neutral PBL. The K expression in the non-neutral condition may be written as (Zilitinkevitch, 1970):

$$K = l^2 \left[\left(\frac{\partial u}{\partial z} \right)^2 + \left(\frac{\partial v}{\partial z} \right)^2 - \alpha \frac{g}{\theta} \frac{\partial \theta}{\partial z} \right]^{\frac{1}{2}}, \quad (14)$$

here Eq. (3) is taken for l , $\alpha = K_h/K_m$ is the ratio of the heat and momentum transfer coefficients whose value is not clear at present, for simplicity, the value of 1 is usually taken in many models, for example, Zhang et al. (1982), we shall take $\alpha = 1$. Eq. (14) instead of Eq. (3) will be used to solve Eqs. (1) and (2).

As mentioned above, $\partial\theta/\partial z$ is derived from solving the motion equations and thermodynamics equation for the steady and homogeneous PBL simultaneously, i. e., $\partial\theta/\partial z$ is derived from Eqs. (14)–(17):

$$\frac{\partial}{\partial z} K \frac{\partial u}{\partial z} + f(v - v_g) = 0 \quad (15)$$

$$\frac{\partial}{\partial z} K \frac{\partial v}{\partial z} - f(u - u_g) = 0 \quad (16)$$

$$\frac{\partial}{\partial z} K \frac{\partial \theta}{\partial z} + S_\theta = 0, \quad (17)$$

where S_θ is the variation rate of the potential temperature caused by radiation, for simplicity, the following scheme is used after Yamamoto et al. (1973):

$$\begin{aligned} S_\theta &= \delta \nu (T - T_s) & (18) \\ \delta &= 1 \quad \text{when } T - T_s > 0 \\ \delta &= 0 \quad \text{when } T - T_s \leq 0 \end{aligned}$$

$\nu = 0.5 \times 10^{-3} \text{ s}^{-1}$, T is temperature, T_s the temperature at the ground. The lower boundary conditions are:

$$u = v = 0; \quad \theta = \theta_s \quad \text{where } z = 0. \quad (19)$$

The upper boundary conditions are:

$$u = u_g, \quad v = v_g; \quad \theta = \theta_h \quad \text{where } z = h, \quad (20)$$

where h is the top of the PBL. We use the conditions (19) and (20) to solve Eqs. (14)–(17) and obtain the wind and potential temperature distributions for the steady, homogeneous and non-neutral PBL. The $\partial\theta/\partial z$ distribution in a real nonsteady and inhomogeneous PBL may have complicated forms. That the $\partial\theta/\partial z$ used to compute K is derived from steady and homogeneous conditions is only an example and the purpose of it is to show the difference between the solutions under the steady and homogeneous conditions and that under the geostrophic momentum approximation. As a computational example, we calculate the wind in the PBL in a trough-ridge system just as the calculation in Zhao (1988).

Assume that $u_g = 15 \text{ m/s}$, $v_g = 5 \text{ m/s}$, $\partial u_g / \partial x = -5 \text{ m s}^{-1} / 10^5 \text{ m}$ in a certain point in the east of a trough. Because of $\partial v_g / \partial x \approx 0$, we can apply the geostrophic momentum approximation. The potential temperature distribution is taken to be the solutions of the Eqs. (14)–(17) when $u_g = 15 \text{ m/s}$, $v_g = 5 \text{ m/s}$, $\theta_h = \pm 10^\circ$, $\theta_s = 0^\circ$, this distribution of θ is shown in Fig. 3.

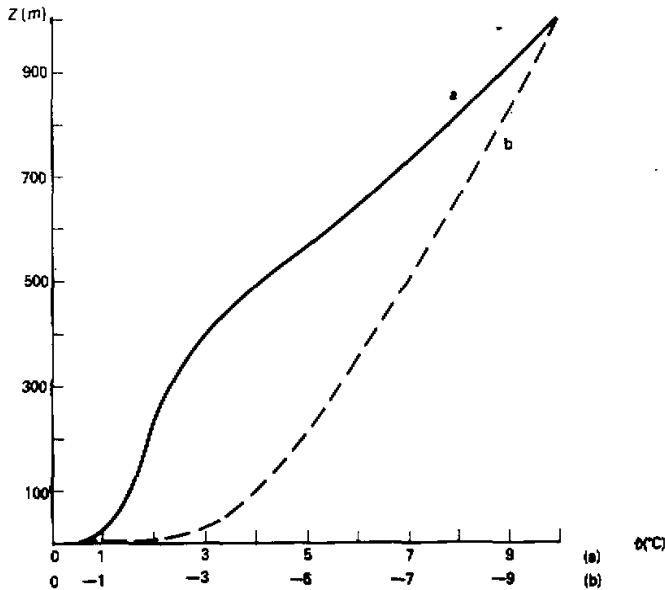


Fig. 3. The distribution of potential temperature, (a) is for stable condition, (b) is for unstable condition.

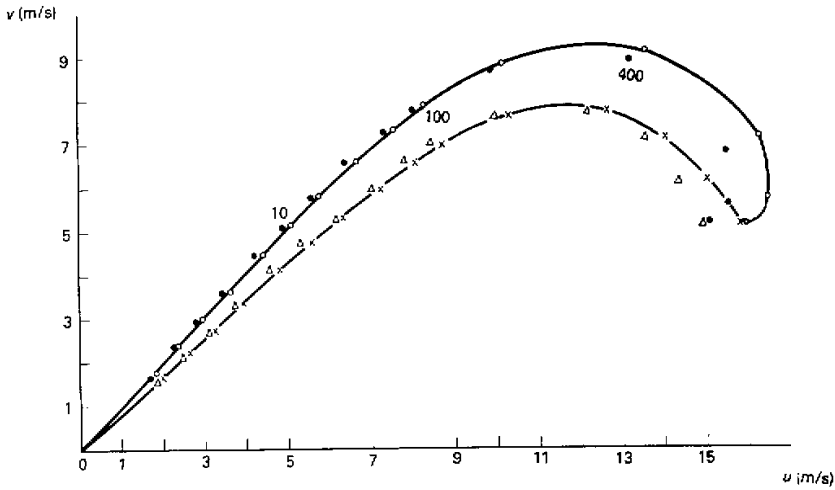


Fig. 4. The calculated wind distribution in the non-neutral PBL with geostrophic momentum approximation, $u_g=15$ m/s, $v_g=5$ m/s, $\partial v_g/\partial x=-5$ m s⁻¹/10⁶ m.
 ○ $\Delta\theta=\theta_h-\theta_s=10^\circ$, geostrophic momentum approximation;
 × $\Delta\theta=-10^\circ$, geostrophic momentum approximation;
 ● $\Delta\theta=10^\circ$, steady and homogeneous solution with $\partial v_g/\partial x=0$;
 △ $\Delta\theta=-10^\circ$, steady and homogeneous solution with $\partial v_g/\partial x=0$.

The wind distribution under the steady and homogeneous conditions which is solved simultaneously with the $\partial\theta/\partial z$ solution and the wind distribution under the geostrophic momentum approximation with $\partial v_g/\partial x=-5$ ms⁻¹/10⁶ m are both shown in Fig. 4. It is found from Eq. (4) that u under the geostrophic momentum approximation are greater than that under the steady and homogeneous conditions. The explanation is the same as given by Zhao (1988). On account of $\partial v_g/\partial x < 0$, $u\partial v_g/\partial x < 0$, it is equivalent to putting $u\partial v_g/\partial x=0$ in Eq. (2) and at the same time to make the fu_g on the right hand side increase, i. e., make u_g increase. This results in the increase of u . This fact shows that the effect of the geostrophic momentum approximation on the wind in the PBL would not be influenced by the stratification, in other words, the geostrophic momentum approximation may be applied in the non-neutral PBL.

On the other hand, we can see that the differences between the solutions with the geostrophic momentum approximation in the cases of unstable and stable stratifications are that the angle between the surface wind and the geostrophic wind is greater in stable condition, and the rate for which the wind approaches the wind at the top of PBL is faster in the stable condition and all of these are in agreement with the characteristics of the unstable and stable PBL. So that the geostrophic momentum approximation does not change the intrinsic characteristics of the unstable and stable PBL. Fig. 5 illustrates the solutions with the geostrophic momentum approximation under the condition that $\Delta\theta=-10^\circ$ incorporating $\partial u_g/\partial t = \pm 5$ m s⁻¹/24 h, $\partial v_g/\partial t = \pm 2$ m s⁻¹/24 h and the same u_g , v_g and

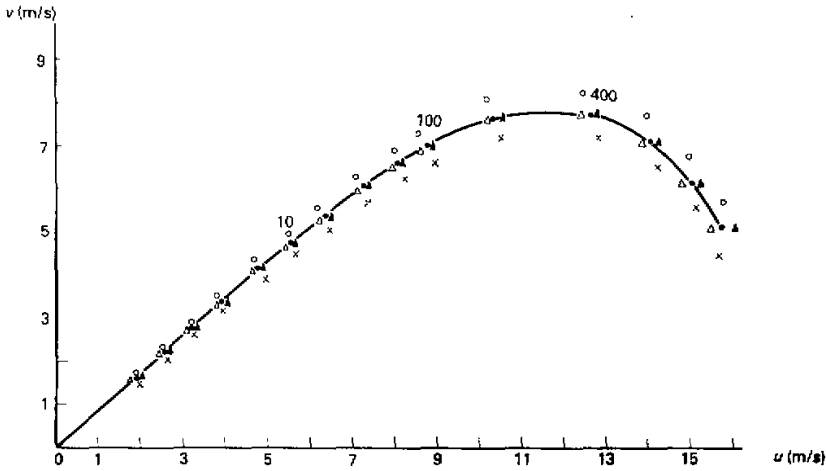


Fig. 5. The wind solutions with the geostrophic momentum approximation,
 $\theta_h = -10^\circ$, $\theta_s = 0^\circ$, $u_g = 15$ m/s, $v_g = 5$ m/s, $\partial v_g / \partial x = -5$ m s⁻¹/10⁴ m,
 ○ $\partial u_g / \partial t = 5$ m s⁻¹/24 h; × $\partial u_g / \partial t = -5$ m s⁻¹/24 h;
 △ $\partial v_g / \partial t = 2$ m s⁻¹/24 h; ▲ $\partial v_g / \partial t = -2$ m s⁻¹/24 h;
 ● $\partial u_g / \partial t = \partial v_g / \partial t = 0$.

$\partial v_g / \partial x$ as in Fig. 4, and the result corresponding to $\partial u_g / \partial t = \partial v_g / \partial t = 0$ but with the same other conditions is also given. It is found that when $\partial u_g / \partial t > 0$, v are greater than that for $\partial u_g / \partial t < 0$; when $\partial v_g / \partial t > 0$, u are less than that for $\partial v_g / \partial t < 0$, these characteristics and their explanations are the same as given in Zhao (1988). This also shows that the geostrophic momentum approximation can be applied successfully both in neutral and non-neutral conditions.

IV. THE ADVANCED CONSIDERATION OF THE STRATIFICATION

The previous results on the non-neutral PBL with the geostrophic momentum approximation are derived in the case that $\partial \theta / \partial z$ is known. In the forecasting of the wind in the PBL based on large scale model, usually θ cannot be given at different heights in the PBL, only the θ at the top of PBL (for example, 850 hPa) and at the surface can be predicted. From the viewpoint of application, we need to determine $\partial \theta / \partial z$. In order to solve this problem, we attempt to solve the Eqs. (1), (2) with the geostrophic momentum approximation in nonsteady and inhomogeneous conditions and the nonsteady thermodynamics equation:

$$\frac{d\theta}{dt} = \frac{\partial}{\partial z} K \frac{\partial \theta}{\partial z} + S_\theta, \quad (21)$$

simultaneously to find the distributions of θ , u , v and K .

Conditions (8) and (9) are used for the upper boundary and condition (10) is used for the lower boundary; the upper boundary condition for θ is:

$$\theta = \theta_h \quad \text{where } z = h, \quad (22)$$

the lower boundary condition for θ is:

$$\theta = \theta_s \quad \text{where } z = 0. \quad (23)$$

The wind and potential temperature can be predicted at the top of PBL by the large scale model, consequently, $d\theta/dt$ then can be calculated. Similarly, $d\theta/dt = \partial\theta/\partial t$ at the surface also can be predicted. The $d\theta/dt$ at different heights in the PBL can then be interpolated. Then Eq. (21) may be solved with Eqs. (1), (2), (14) simultaneously to find u , v , $\partial\theta/\partial z$ and K . Of course, this method to find $\partial\theta/\partial z$ is not accurate enough, however, we are concerned with finding the distribution of the wind but not finding the accurate distribution of θ , that we find θ distribution is only for calculating the K affected by the stratification. The numerical experiments show that the difference between the results neglecting the $d\theta/dt$ term and not in Eq. (21) is not obvious (see Fig. 6). This means that the previous treatment for $d\theta/dt$ is permitted. Therefore, the wind distribution in the PBL with the geostrophic momentum approximation may be computed by solving Eqs. (1), (2), (14), (21) simultaneously. By the way, there is the possibility to give the three dimensional initial and boundary conditions in small scale problems, so that Eq. (21) may be solved precisely for those problems, but it is not true for the large scale model.

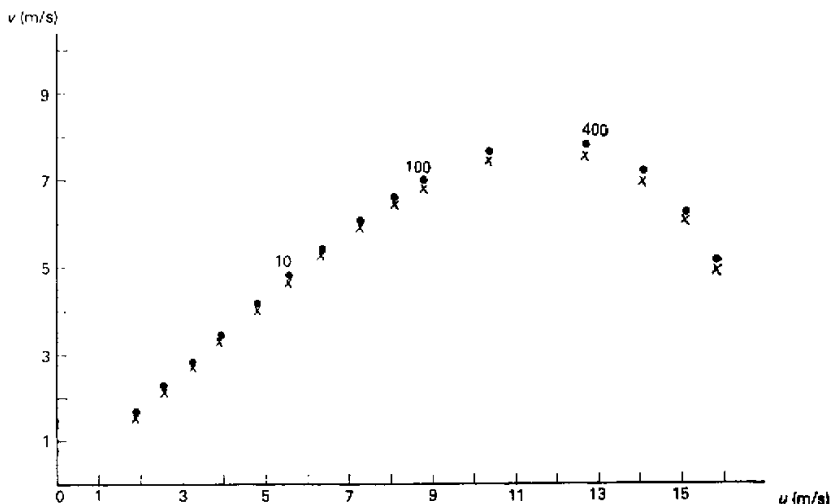


Fig. 6. The wind solutions with the geostrophic momentum approximation,
 $\theta_h = -10^\circ$, $\theta_s = 0^\circ$, $u_g = 15$ m/s, $v_g = 5$ m/s, $\partial v_g/\partial x = -5$ m s⁻¹/10⁶ m,
 $\partial\theta/\partial z$ is solved from Eqs. (1), (2), (14), (21),
 · are for $d\theta/dt = 5^\circ/24$ h; x are for $d\theta/dt = -5^\circ/24$ h.

As an example, we assume that $u_g = 15$ m/s, $v_g = 5$ m/s, $\partial v_g/\partial x = -5$ m s⁻¹/10⁶ m, $\theta_h = -10^\circ$, $\theta_s = 0^\circ$, $d\theta/dt = \pm 5^\circ/24$ h at different heights, the solutions of Eqs. (1), (2),

(14), (21) with the geostrophic momentum approximation are shown in Fig. 6, the results are compared with the corresponding case in Fig. 4 ($d\theta/dt=0$). It is shown that the two solutions with $d\theta/dt = \pm 5^\circ/24$ h are approached each other and the solution corresponding to $d\theta/dt=0$ is just between them (not illustrated). This shows that the effect of $d\theta/dt$ is not important in the case of $d\theta/dt=5^\circ/24$ h, $d\theta/dt=0$ may be taken approximately.

Theoretically the inclusion of $dt/d\theta$ should be better if $\left| \frac{d\theta}{dt} \right|$ is greater.

Now we consider the effects of the baroclinity and non-neutral condition simultaneously, the symbol '▲' in Fig. 2 represents the results when $\theta_h = -10^\circ$, $\theta_s = 0^\circ$, $\partial u_g/\partial t = -5$ m s⁻¹/24 h are assumed and with the same vertical distribution of the geostrophic wind as in the other curves in Fig. 2. If the results are compared with other curves in Fig. 2 which represent the results in the case of $\partial u_g/\partial t = -5$ m s⁻¹/24 h in the neutral but baroclinic condition, then we can see that in the former case, the wind approaches its value at the upper boundary slower than that in the latter case, and the angle between the surface wind and the wind at the upper boundary is smaller for the former case. That means the characteristics for the baroclinity and non-neutral conditions are all reflected, i. e., the geostrophic momentum approximation can be applied in the baroclinic and non-neutral conditions.

V. THE APPLICATION TO THE PBL OVER SEA SURFACE

Zhao (1987) had applied the model of steady, homogeneous and barotropic PBL to the condition over sea surface, the equations were (15), (16), (3)-(6) in which the roughness was a function of friction velocity. For the rough flow,

$$z_0 = 0.0144 \frac{u_*^2}{g}. \quad (24)$$

The upper boundary condition was $u = u_g$, $v = v_g$; the lower boundary was located at a certain low height near the mean level of sea surface and the condition for the lower boundary was:

$$\frac{\partial V}{\partial z} = \frac{u_*}{k(z+z_0)}, \quad (25)$$

where $V = \sqrt{u^2 + v^2}$. The model resulted in the wind distribution and some boundary layer parameters which were in agreement with observations. At present, it is not difficult to extend that model to the non-neutral condition with the geostrophic momentum approximation. The equations are (1), (2), (14), (21), the lower boundary condition for the wind is still (25). Because the lower boundary is located at a very low height (the grid system is the same as Zhao (1987), the lowest grid point is located at 0.25 m), the stability at that height may be treated as neutral. The upper boundary conditions for the winds are (8), (9); for the potential temperature are $\theta = \theta_h$. The lower boundary is not located at surface, so $\theta \neq \theta_0$ (θ_0 is the θ value at the surface). We utilize the temperature profile in the surface layer for which the correcting function may be neglected on account of such a low height and obtain:

$$\theta_1 = \theta_0 + \frac{T_*}{k} \ln \frac{z_1}{z_{0h}}, \quad (26)$$

where θ_1 is the potential temperature at the lower boundary ($z_1=0.25$ m), Eq. (26) is used as the lower boundary condition, k is the Karman constant, $T_* = -H/c_p \rho u_*$, the friction temperature, H the turbulent heat flux, z_{0h} the height at which the potential temperature takes the value at the surface, according to Brutsaert (1982),

$$z_{0h} = 7.4 z_0 e^{-2.46 \left(\frac{u_* z_0}{\nu} \right)^{1/4}}. \quad (27)$$

T_* in Eq. (26), z_0 , u_* in Eq. (27) are all the quantities requiring to be determined from the solutions u , v and θ of the equations and the lower boundary conditions (25), (26) also contain the parameters depending on the solutions of the equations. We solve the equations as follows.

From the wind and temperature profiles in the surface layer (Panofsky and Dutton, 1984):

$$V = \frac{u_*}{k} \left[\ln \frac{z}{z_0} - \psi_m \left(\frac{z}{L} \right) \right], \quad (28)$$

$$\theta - \theta_0 = \frac{T_*}{k} \left[\ln \frac{z}{z_{0h}} - \psi_h \left(\frac{z}{L} \right) \right], \quad (29)$$

where ψ_m , ψ_h are the known functions of z/L , L is the Monin-Obukhov length $L = u_*^2 T / g h T_*$, the u_* and L can be calculated from the values V and θ at z_0 , a certain height in the surface layer (for example, 10 m) in Eqs. (28), (29), and V and θ at z_0 can be computed from the approximate solutions of Eqs. (1), (2), (14), (21) in each step when these equations are solved by the successive approximation method. The approximate solutions at the first step may choose some appropriate values, the successive approximation method by Zhao (1987, 1988) can obtain the solutions which satisfies both Eqs. (1), (2), (14), (21) and (25)-(29).

Assuming $\theta_h = -10^\circ$, $\theta_0 = 0^\circ$, $\partial v_g / \partial x = -5 \text{ m s}^{-1} / 10^6 \text{ m}$, $u_g = 15 \text{ m/s}$, $v_g = 5 \text{ m/s}$, $d\theta/dt = -5^\circ/24 \text{ h}$, we get the solutions as shown in Fig. 7, in which the solutions in the steady and homogeneous conditions with the same u_g , v_g , θ_h and θ_0 are also illustrated besides the solutions with the geostrophic momentum approximation. It is found that the characteristic that the wind speeds at lower heights are greater over sea is still retained, the angle between the surface wind and the geostrophic wind is still less than that over land. This means that the geostrophic momentum approximation does not change the main characteristics of the wind in the PBL over sea, only the characteristics with the geostrophic momentum approximation are added to the original characteristic over sea, i. e., when $\partial v_g / \partial x < 0$, the u is stronger. All of these show that the geostrophic momentum approximation can be applied successfully over sea surface.

When the flow is smooth, we can solve the similar problem without difficulty with the same treatment as in Zhao (1987).

VI. THE CONCLUSIONS

After the K expressions are treated by the modern PBL theory, the W-B's boundary

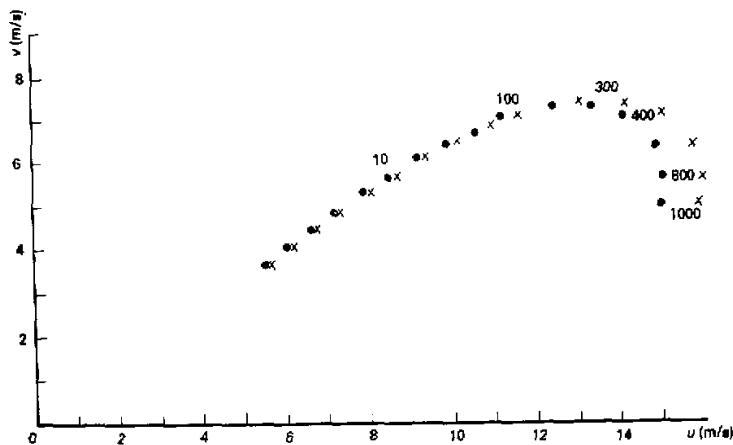


Fig. 7. The wind distribution in the non-neutral PBL over sea,
 × $\theta_h = -10^\circ$, $\theta_0 = 0^\circ$, $\partial v_g / \partial x = -5 \text{ m s}^{-1} / 10^4 \text{ m}$, $u_g = 15 \text{ m/s}$, $v_g = 5 \text{ m/s}$,
 $d\theta/dt = -5^\circ/24 \text{ h}$ with the geostrophic momentum approximation,
 • $\theta_h = -10^\circ$, $\theta_0 = 0^\circ$, $u_g = 15 \text{ m/s}$, $v_g = 5 \text{ m/s}$, $d\theta/dt = 0$ with steady and
 homogeneous conditions.

layer geostrophic momentum approximation theory may not only be used to solve numerically the equations for the PBL to obtain the wind distribution in the neutral PBL, but also be used to calculate the wind distribution in non-neutral PBL incorporating the thermodynamics equation. For the baroclinic PBL, the geostrophic momentum approximation may also be applied. Furthermore, it can be applied to the PBL over sea surface if the lower boundary condition is changed. The work in this paper improves the W-B's primary work. The uses of the models in this paper are: the winds at different heights in the PBL may be diagnosed by these models as long as the geostrophic wind, its spatial distribution and temporal tendency, the temperature and its variation at the top and bottom of the PBL are predicted by the large scale model. The aim of this research is to study the wind distribution, and the finding of the temperature distribution is only for calculating the K . The computation of $\partial\theta/\partial z$ is not rigorous in this paper. However, as the numerical experiments show, its effect on the wind is not important. The models in this paper can be applied to the forecasting of the wind in the PBL over land or sea.

REFERENCES

- Brutsaert, W.H. (1982), Evaporation into the atmosphere, D. Reidel Publishing Co., 122-123.
 Deardorff, J.W. and Mahrt, L. (1982), On the dichotomy in theoretical treatments of the atmospheric boundary layer, *J. Atmos. Sci.*, 29:2096-2103.
 Estoque, M.A. (1973), Numerical modeling of the PBL, in: 'Workshop on Micrometeorology', *Amer. Meteor. Soc.*, 217-270.
 Liu, Q. and Qin, Z. (1986), Dynamics of nonlinear baroclinic Ekman boundary layer, *Adv. Atmos. Sci.*, 3:421-431.
 Panofsky, H.A. and Dutton, J.A. (1984), *Atmospheric Turbulence, Models and Methods for Engineering Applica-*

- tions, Wiley-Interscience, 133-148.
- Qin, Z., Liu, Q. and Feng, S. (1986), The numerical experiments on the nonlinear dynamical diagnosed model of the wind field in the atmospheric boundary layer over sea, *Acta Oceanologica Sinica*, **8**: 678-685. (in Chinese)
- Wu, R. and Blumen, W. (1982), An analysis of Ekman boundary layer dynamics incorporating the geostrophic momentum approximation, *J. Atmos. Sci.*, **39**: 1774-1782.
- Yamamoto, G., Shimanuki, A., Aida, M., Yasuda, N. (1973), Diurnal variation of wind, temperature field in the Ekman layer, *J. Met. Soc. Japan*, **51**:377-387.
- Zhang, D. and Anthes, R.A. (1982), A high-resolution model of the PBL-sensitivity tests and comparisons with SESAME-79 data, *J. App. Met.*, **21**:1594-1609.
- Zhao, M. (1987), A numerical model of the neutral atmospheric boundary layer with the varying roughness, *Sci. Atmos. Sinica*, **11**:247-256. (in Chinese)
- Zhao, M. (1988), A numerical experiment of the atmospheric boundary layer with geostrophic momentum approximation, *Adv. Atmos. Sci.*, **5**:47-56.
- Zilitinkevitch, S.S. (1970), *The dynamics of the atmospheric boundary layer*, Gidrometeoizdat, 288 pp. (in Russian)

